analytical chemistry

Article

Cite This: *Anal. Chem.* XXXX, XXX, XXX−XXX

pubs.acs.org/ac

Real-Time and In-Situ Monitoring of H_2O_2 Release from Living Cells by a Stretchable Electrochemical Biosensor Based on Vertically Aligned Gold Nanowires

Quanxia Lyu,[†,‡] Qingfeng Zhai,[†,‡] Jennifer Dyson,[‡,§,∥] Shu Gong,[†,‡] Yunmeng Zhao,[†,⊥] Yunzhi Ling,[†,⊥] Ramya Chandrasekaran,[†,‡] Dashen Dong,[†,‡] and Wenlong Cheng*[,†,‡,§,⊥]

[†]Department of Chemical Engineering, Monash University, Clayton, Victoria 3800, Australia

[‡]New Horizon Research Centre, Monash University, Clayton, Victoria 3800, Australia

[§]Monash Institute of Medical Engineering, Monash University, Clayton, Victoria 3800, Australia

[∥]Department of Biochemistry & Molecular Biology, Biomedicine Discovery Institute, Clayton, Victoria 3800, Australia

[⊥]The Melbourne Centre for Nanofabrication, Clayton, Victoria 3800, Australia

Supporting Information

ABSTRACT: Traditional electrochemical biosensing electrodes (e.g., gold disk, glassy carbon electrode, etc.) can undergo sophisticated design to detect chemicals/biologicals from cells. However, such electrodes are typically rigid and nonstretchable, rendering it challenging to detect cellular activities in real-time and in situ when cells are in mechanically deformed states. Here, we report a new stretchable electrochemical cell-sensing platform based on vertically aligned gold nanowires embedded in PDMS (v-AuNWs/PDMS). Using H_2O_2 as a model analyte, we show that the v-AuNWs/PDMS electrode can display an excellent sensing performance with a wide linear range, from 40 μM to 15 mM, and a high sensitivity of 250 mA/cm^2/M at a potential of −0.3 V. Moreover, living cells can grow directly on our stretchable high-surface area electrodes with strong adhesion, demonstrating their excellent biocompatibility. Further cell stimulation by adding chemicals induced H_2O_2 generation, which can be detected in real-time and in situ using our v-AuNWs/PDMS platform for both natural and stretched states of cells. Our results indicate the v-AuNWs/PDMS electrochemical biosensor may serve as a general cell-sensing platform for living organisms under deformed states.

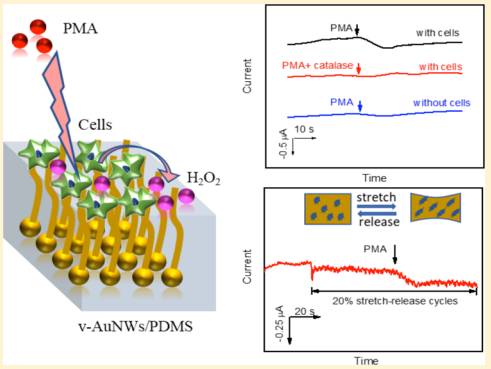

Hydrogen peroxide (H_2O_2), as one of the most common representatives of reactive oxygen species (ROS), is considered to be a "necessary evil" for mammalian cell signalings.[1] On one side, it is related to diverse cellular behaviors, including cell proliferation, differentiation, and migration under physiological conditions.[2−4] On the other side, overgeneration of H_2O_2 may disrupt the cellular redox homeostasis imposing oxidative stress on biotissues. Consequently, excessive levels of H_2O_2 are associated with various pathological events, such as cancer, cardiovascular dysfunctions, aging, Parkinson's disease, and Alzheimer's disease.[5−7] Therefore, it is imperative to develop sensitive and high cost-effective analytical techniques for real-time monitoring of H_2O_2 from living organisms in real time and in situ.

To date, several novel electrochemical biosensors have been developed for detection of cellular secreted H_2O_2 based on various materials, such as graphene,[8−11] reduced graphene oxide,[12] MoS_2 nanoparticles,[13] AuCu nanowires,[14] MnO_2 nanowires/nanosheet,[15,16] ZnO nanosheet,[17] carbon nanotube,[18] protein microarray-modified Au-TiO_2,[19] manganese dioxide,[20] and porous polymer hydrogels.[21] Notably, these reported sensors are all based on planar and rigid electrodes, albeit a flexible biosensor was reported but without demonstration of the detection under mechanical strain.[22] It would be of great benefit if H_2O_2 detection could be realized when cells are deformed, which may lead to next-generation soft wearable/implantable biosensors conformal to elastic and the curved human body for better health monitoring. Encouragingly, it has been recently reported that cellular released nitric oxide (NO) could be detected via a flexible and stretchable electrochemical electrode based on nanostructured gold.[23−26] Despite the advances, however, much still needs to be addressed for other important biomarkers, such as cellular released H_2O_2, which may require novel electrode structural design.

Recently, our group has established a novel soft sensing platform based on vertically aligned gold nanowires (v-AuNWs).[27−29] The stretchable v-AuNWs could maintain its conductivity up to 800% mechanical strain under optimum

Received: June 7, 2019
Accepted: September 24, 2019
Published: September 24, 2019

DOI: 10.1021/acs.analchem.9b02610
Anal. Chem. XXXX, XXX, XXX−XXX

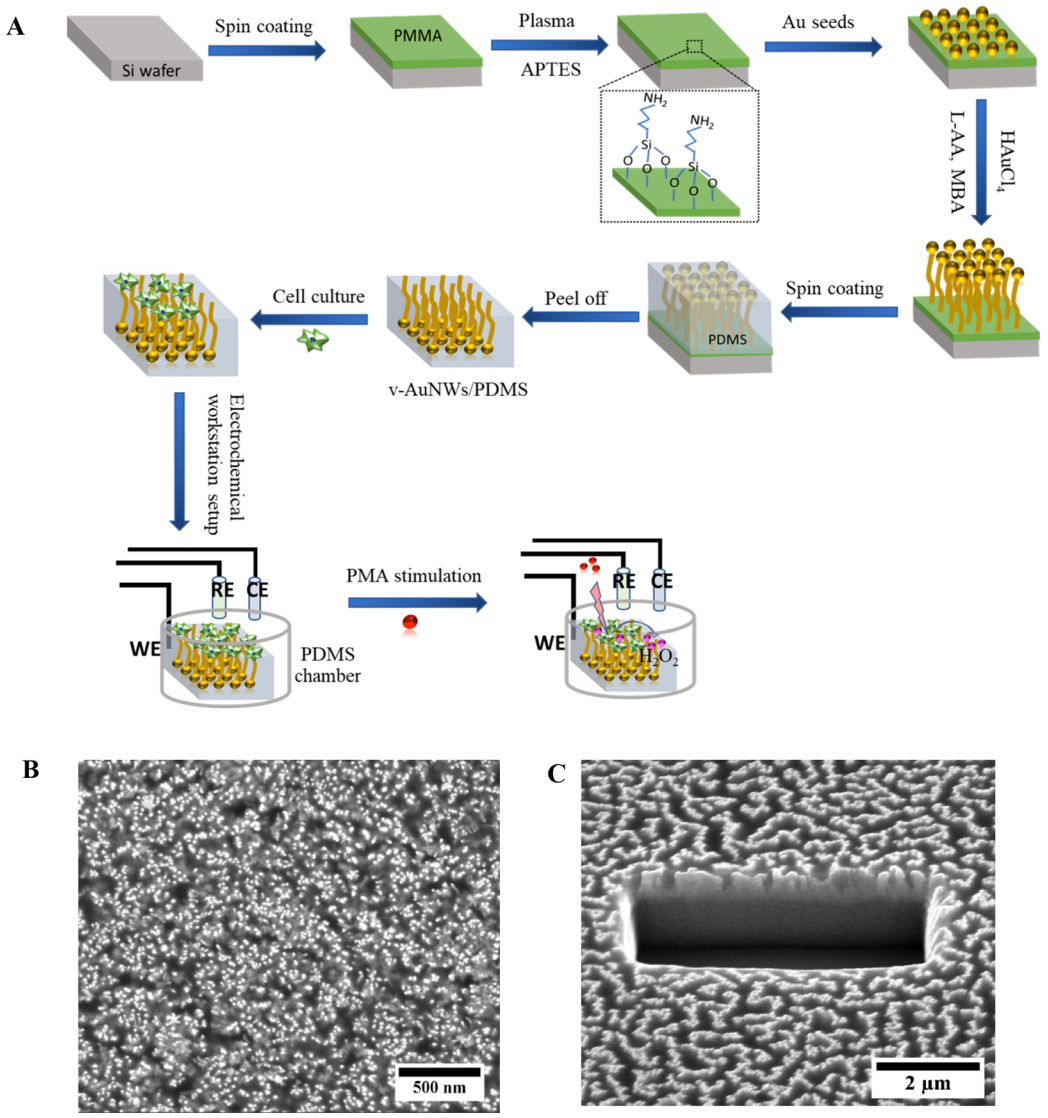

Figure 1. Fabrication and characterization of the stretchable v-AuNWs/PDMS electrodes: (A) schematic of the fabrication process for the stretchable v-AuNWs/PDMS electrodes, (B) top-view SEM image of the v-AuNWs/PDMS electrode; and (C) cross-section SEM image of the vertically aligned AuNWs.

conditions.[30] This property in conjunction with the high conductivity, high surface area, and facile surface modification, allowed for v-AuNWs stretchable electrochemical electrodes toward H_2O_2 and glucose.[31,32] This motivated us to further explore their potential application in real time and in situ monitoring of H_2O_2 released from living cells. This study shows that v-AuNWs electrode is also a biocompatible electrode enabling direct cell growth. The released H_2O_2 from living cells upon chemical stimulation can be detected both under nonstrained and highly stretched states. Our results indicate the potential of our v-AuNWs as soft stretchable electrochemical sensing platforms for conformal cell monitoring under mechanical deformations.

EXPERIMENTAL SECTION

Materials. (3-Aminopropyl) triethoxysilane (APTES), gold(III) chloride hydrate ($HAuCl_4$), sodium borohydride ($NaBH_4$), sodium citrate dihydrate, L-ascorbic acid (L-AA), 4-mercaptobenzoic acid (MBA), potassium ferrocyanide (III) ($K_3Fe(CN)_6$), potassium hexacyannoferrate ($K_4Fe(CN)_6$), potassium chloride (KCl), hydrogen peroxide (30% H_2O_2), phosphate buffered saline (PBS tablet), propidium iodide (PI), catalase, and phorbol 12-myristate 13-acetate (PMA) were purchased from Sigma−Aldrich. DPBS, DMEM, FBS, TrypLE Express Enzyme, Calcein AM, penicillin, and streptomycin were purchased from Thermo Scientific. Silicon wafer ⟨100⟩ was purchased from Electronics and Materials Corporation Limited, Japan. Poly(methyl methacrylate) (PMMA 950 A6) was purchased from MicroChem Corp. (Westborough, MA, USA). PDMS base and curing agent (Sylgard 184) were purchased from Dow Corning. All the purchased chemicals were at analytical grade and used as received. Milli-Q water (resistivity of >18 MΩ cm^{-1}) was used throughout all the experiments in this work.

Fabrication of the Stretchable v-AuNWs/PDMS Film. The v-AuNWs/PDMS film was fabricated via a seeded growth method. First of all, a thin layer of PMMA was spin-coated on the surface of a silicon wafer at 3000 rpm for 45 s and baked at 180 °C for 2 min. Then, the PMMA-coated Si wafer underwent an O_2 plasma treatment for 5 min, followed by

DOI: 10.1021/acs.analchem.9b02610
Anal. Chem. XXXX, XXX, XXX−XXX

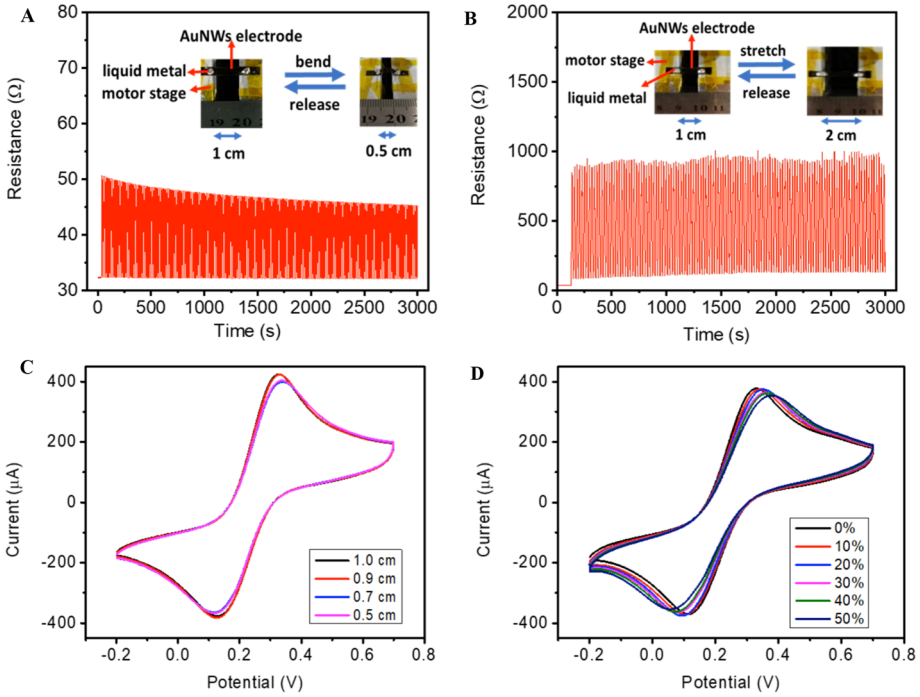

Figure 2. Electrical and electrochemical characterization of the stretchable v-AuNWs electrode. (A) The resistance changes of the v-AuNWs electrode (active area = 1.0 cm × 0.5 cm) under applied cyclic bending (250 cycles). (B) The resistance changes of the v-AuNWs electrode under applied cyclic strains from 0% to 100% (150 cycles). (C) Cyclic voltammograms of 5 mM $K_3[Fe(CN)_6]/K_4[Fe(CN)_6]$ at a scan rate of 0.05 V/s on the v-AuNWs electrode under different levels of bending. (D) Cyclic voltammograms of 5 mM $K_3[Fe(CN)_6]/K_4[Fe(CN)_6]$ at a scan rate of 0.05 V/s on the v-AuNWs electrode under different levels of strains.

amine modification by immersion into APTES for 2 h. Next, the modified PMMA was immersed in citrate-stabilized gold seeds for 2 h. The gold seeds were prepared by adding 0.5 mM sodium citrate and 6 mM $NaBH_4$ solution to 0.25 mM $HAuCl_4$ solution under stirring. The gold seed anchored PMMA was then soaked in AuNWs growth solution, which was composed of 12 mM $HAuCl_4$, 1.1 mM MBA ligand, and 30 mM L-AA reducing agent in ethanol/water mixed solvent (v/v 1:1.2). After immersion in growth solution for 3 min, the modified substrate was rinsed with ethanol and dried by blowing with N_2. After these steps, the PMMA/silicon wafer was spin-coated with a mixture of PDMS base and curing agent (w:w 10:1) at 350 rpm for 35 s. The coated PDMS precursor was then put into an oven at 60 °C overnight. Finally, the cured PDMS, together with the v-AuNWs, was peeled off from the substrate.

Characterization of the v-AuNWs/PDMS Film. *Morphology Properties.* SEM images were obtained from FEI Nova NanoSEM 450 FEG SEM. Cross-section SEM images were taken by FEI Helios Nanolab 600 FIB-SEM.

Electrical Characterization. Two sides of a patch of v-AuNWs/PDMS film were fixed on the moving stage of a sliding motor (Thorlabs Model LTS150/M). The patch then was connected to the electrochemical workstation (Versa-STAT3, Princeton Applied Research) via two thin copper wires sealed with liquid metal. The dimensions of the final active electrode area were 1.0 cm × 0.5 cm. The resistance of the v-AuNWs patch was continuously measured for hundreds of cycles by the electrochemical workstation under different levels of bending and cyclic strains. As for the bending test, the distance of the two ends of the v-AuNWs film decreased from 1.0 cm to 0.5 cm, along with the increased levels of bending. As for the stretchability test, the distance of the two sides of the v-AuNWs electrode increased from 1.0 cm to 2.0 cm with the corresponding applied strain at 0% to 100%.

Electrochemical Characterization. The electrochemical properties were characterized using the standard three-electrode system. The v-AuNWs/PDMS film fabricated above was used as the working electrode. Ag/AgCl was used as the reference electrode and platinum wire as the counter electrode. The electrochemical performance of the v-AuNWs/PDMS electrode in 1 M H_2SO_4 and in 5 mM $Fe(CN)_6^{3-/4-}$ at different levels of bending and stretching were recorded using cyclic voltammetry.

Calibration of the v-AuNWs Electrode for H_2O_2. A series of concentrations of H_2O_2 were prepared by diluting the commercial 30% H_2O_2 solution gradually. Calibration for H_2O_2 was conducted by adding H_2O_2 drops in a chamber containing PBS solution (pH 7.4) with the three electrodes inside the solution. The potential vs Ag/AgCl electrode was set at −0.3 V for the amperometric detection for H_2O_2.

Cell Culture and Imaging. *Cell Culture.* MDA-MB-231 (breast cancer cell line) cells were cultured using DMEM medium supplemented with 10% fetal bovine serum and 1% penicillin and streptomycin. Culture flasks containing the MDA-MB-231 cells were kept at 37 °C in a humidified incubator with 95% air and 5% CO_2. As for the cell detection assay, the MDA-MB-231 cells at an approximate density of 2×10^5 cells/cm^2 were seeded on the v-AuNWs/PDMS electrode. The electrode was surrounded with a PDMS chamber as a reservoir to hold medium or solution. Before seeding, the chamber together with the AuNWs film were sterilized with 75% ethanol and ultraviolet (UV) exposure in a tissue culture fume hood. After sterilization, the chamber was washed by PBS solution and balanced by prewarmed medium. After 24 h of plating, the cells were used for H_2O_2 releasing studies.

DOI: 10.1021/acs.analchem.9b02610
Anal. Chem. XXXX, XXX, XXX−XXX

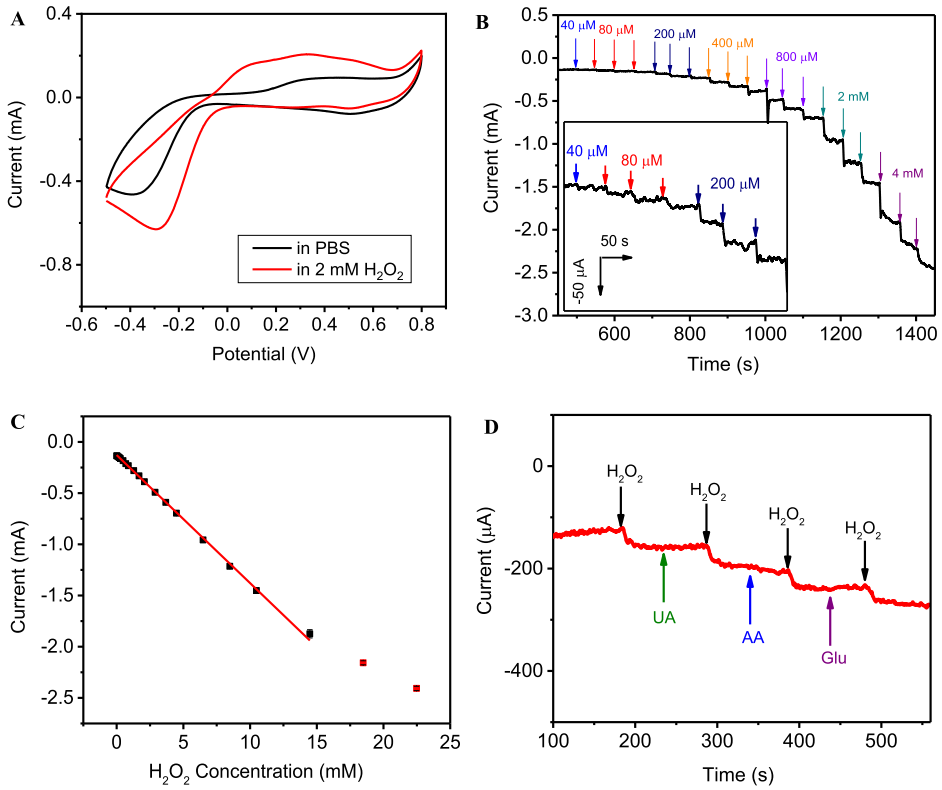

Figure 3. Electrochemical sensing of H_2O_2 by the v-AuNWs electrode. (A) Cyclic voltammograms of the AuNWs electrode for PBS buffer without (black line) and with 2 mM H_2O_2 (red line). (B) Chronoamperometric responses of the AuNWs electrode to increasing H_2O_2 concentrations poised at −0.3 V vs Ag/AgCl. (C) Calibration curve for the AuNWs electrode between the current and corresponding concentrations of H_2O_2. (D) Amperometric responses of the AuNWs electrode to successive additions of 0.5 mM H_2O_2, 1.0 mM UA (urea acid), 1.0 mM AA (ascorbic acid), and 1.0 mM Glu (glucose) at −0.3 V.

Fluorescent Staining and Cell Imaging. In order to assess the biocompatibility of the fabricated v-AuNWs/PDMS film, MDA-MB-231 cells were cultured on a small patch of the film (0.5 cm × 0.5 cm) for 24 h after passage. After removal of the culture medium in the culture flask, fluorescent live/dead cell dyes Calcein-AM (2 μg/mL) and PI (3 μg/mL) were added to the cultured MDA-MB-231 cells on v-AuNWs/PDMS film. Then, after 20 min of incubation in the cell incubator, the stained cells were observed and imaged using a fluorescent microscope (Nikon, Model ECLIPSE Ts2).

RESULTS AND DISCUSSION

Fabrication and Characterization. The v-AuNWs/PDMS film was prepared through a seeded growth method (Figure 1A). In brief, PMMA was spun onto silicon water, followed by O_2 plasma to render surface rich with hydroxyl groups. Further treatment with silane agent APTES allowed for surface medication with amine groups, which could attract negatively charged gold seeds from colloidal solution. Upon short-time immersion in the growth solution, v-AuNWs spontaneously formed. A layer of PDMS precursor then was spin-coated onto v-AuNWs and cured in a 60 °C oven overnight. This step allowed for peeling off of v-AuNWs from the substrate. Typical top-view and cross-sectional SEM images (see Figures 1B and 1C) proves the successful fabrication of the densely packed v-AuNWs.

Electrical Responses to Mechanical Deformation. The electrical properties of the as-fabricated v-AuNWs were thoroughly evaluated under various mechanical deformation bending, stretching, and repeated loads. As for the bending test, the two ends of the electrode were mounted onto the stepper motor and then connected to the electrochemical workstation. Figure 2A shows the resistance changes of the v-AuNWs electrode under the applied cyclic bending. The resistance of the electrode film changed from 32 Ω to 50 Ω in the first cycle of bending. After 250 bending cycles, the resistance of the film went back to its original level. Figure 2B shows the resistance changes of the v-AuNWs electrode under applied cyclic strains from 0% to 100% and then back to 0%. The resistance of the electrode film changed from 32 Ω to 830 Ω with excellent resistance recovery upon strain release. These results show that our v-AuNWs electrode possesses high conductivity, even in a severely deformed state, which is a prerequisite for the application as the electrochemical electrode. Unlike conventional gold films, our v-AuNWs film exhibited small nanocracks, as shown in the SEM images under stretched state (see Figure S1 in the Supporting Information). The tiny cracks enabled reliable conductivity recovery upon strain release.

Electrochemical Properties. The fabricated v-AuNWs/PDMS electrode was cleaned and activated by cyclic voltammetry in 1 M H_2SO_4 for 20 cycles at a scan rate of 0.1 V/s. Figure S2 in the Supporting Information presents a typical voltammogram with the appearance of oxidation peaks after 1.3 V and a characteristic reduction peak at a potential of ~0.9 V. The charges during the reduction process is calculated as 3.19×10^{-3} C by integration of the reduction peak. The required charge for the reduction of a monolayer of gold oxide is 386 μC/cm;[2,23,31,33] therefore, the electrochemical active surface area (EASA) of the v-AuNWs/PDMS electrode is

DOI: 10.1021/acs.analchem.9b02610
Anal. Chem. XXXX, XXX, XXX−XXX

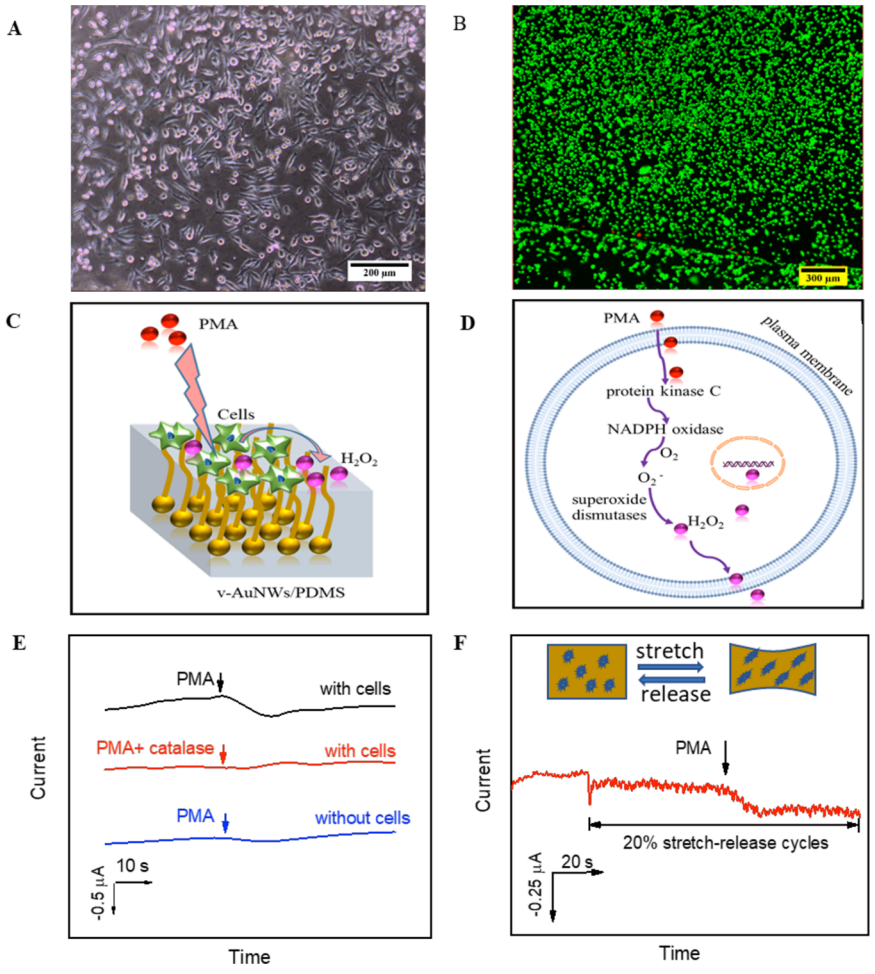

Figure 4. Biocompatibility of the v-AuNWs electrode and real-time monitoring of H_2O_2 from the living cells. (A) Microscopic image of MDA-MB-231 (breast cancer) cells cultured on the v-AuNWs/PDMS electrode. (B) Fluorescent image for the live/dead assay (Calcein-AM stained (green) and PI stained (red)). (C) Scheme for monitoring of released H_2O_2 by the v-AuNWs electrode upon chemical (PMA) stimulation. (D) Scheme of proposed cellular processes to generate H_2O_2 upon chemical stimulation. Monitor of H_2O_2 released from cells upon the addition of stimulant by the v-AuNWs electrode under (E) the original state and (F) 20% stretch-release cycles.

estimated to be 8.2 cm^2. This is ~16 times greater than the corresponding geometrical area (0.5 cm^2). Such a high EASA is expected, given the unique v-AuNWs with high porosity in the matrix.

In order to examine the electrochemical performance of the v-AuNWs/PDMS electrode under mechanically deformed states, the typical redox probe of $K_3[Fe(CN)_6]/K_4[Fe(CN)_6]$ was used. Figure 2C presents the cyclic voltammograms of 5 mM $K_3[Fe(CN)_6]/K_4[Fe(CN)_6]$ at a scan rate of 0.05 V/s on the electrode under different levels of bending. Note that the line profiles exhibit negligible responses to the different bending curvatures. Figure 2D shows that the cyclic voltammograms of 5 mM $K_3[Fe(CN)_6]/K_4[Fe(CN)_6]$ at a scan rate of 0.05 V/s on the electrode under different levels of tensile strains from 0% to 50%. Note that the redox peak currents only decrease ~5.8% and peak-to-peak separation increases from 205 mV to 320 mV, even under 50% strain. The excellent performance for both bending and stretching tests prove the high electrochemical stability of our v-AuNWs electrode, which is important for subsequent cell-biosensing under mechanically deformed states. Moreover, the cyclic voltammograms of 5 mM $K_3[Fe(CN)_6]/K_4[Fe(CN)_6]$ were also recorded by the v-AuNWs electrode after undergoing different cycles of 50% stretching/releasing. From Figure S3 in the Supporting Information, one can see that, even after 700 stretching/releasing cycles at 50% strain, the peak−peak separation of the CVs and redox currents shows no significant changes. After 1000 stretching/releasing cycles, there are some observable variations, with the peak-to-peak separation increasing from 190 mV to 350 mV and reduction current decreasing by 15%. These variations may attribute to the established structural changes for the v-AuNWs electrode, as shown in Figure S4 in the Supporting Information. The generation of more cracks in the v-AuNWs electrode might explain the deterioation of the electrochemical sensing performance.

Sensing Performance toward H_2O_2. The electrochemical detection performance toward H_2O_2 by the v-AuNWs/PDMS electrode was further investigated. Figure 3A shows the comparison of the CVs with and without the presence of H_2O_2. It could be clearly seen that there was remarkable increase of the reduction peak at the potential of −0.3 V in 2 mM H_2O_2, compared with that in pure PBS buffer. Therefore, −0.3 V was chosen as the working potential in this work.

Figure 3B shows the staircase-like chronoamperometric responses to H_2O_2 with increasing concentrations. The v-AuNWs/PDMS biosensor started to respond to H_2O_2 after

DOI: 10.1021/acs.analchem.9b02610
Anal. Chem. XXXX, XXX, XXX−XXX

reaching a concentration of ~40 μM. With the following successive addition, the corresponding currents increased accordingly, which follows a linear relationship between the concentration of H_2O_2 and the Faradaic current with a correlation coefficient (R^2) of 0.999, as shown in Figure 3C. The estimated linear detection range is 40 μM to 15 mM, with a detection sensitivity of 250 mA/cm^2/M. The calculated detection limit (LOD) is ~12 μM (S/N = 3). Compared to the literature regarding H_2O_2 detection from living cells with rigid electrodes, our stretchable v-AuNWs/PDMS electrode shows a relatively wider linear range and high sensitivity (see Table S1 in the Supporting Information). This wide range of detection may due to the high electrochemically active surface area demonstrated above. With a higher active area involved, the more H_2O_2 molecules are in contact with sensing electrodes, thereby leading to a wider sensing region. In contrast, the LOD in our system is not superior to other electrodes reported in the literature (see Table S1). Nevertheless, our v-AuNWs is stretchable, which is beneficial for detection from soft living organisms under mechanical deformation. Importantly, the sensing performance under a stretched state was not affected much, showing the similar sensitivity to that under the nondeformed state (Figures S5 and S6 in the Supporting Information).

To assess the reproducibility of the v-AuNWs electrode, amperometric measurements were conducted on five different v-AuNWs electrodes with the same geometric area (0.5 cm × 0.5 cm) and chronoamperometric measurements were conducted on the same v-AuNWs electrode for three times. Figure S7 in the Supporting Information shows that the electrochemical responses to the same amount of H_2O_2 for the different v-AuNWs electrodes is reproducible, with a relative standard deviation (RSD) of 5.4%. In addition, our v-AuNWs electrodes exhibit consistent chronoamperometric responses to different concentrations of H_2O_2 for the repeating experiments on the same v-AuNWs electrode (Figure S8 in the Supporting Information), demonstrating the excellent reproducibility. We also tested the storage stability of the v-AuNWs electrode by continuously detecting the fixed amount of H_2O_2 by a same v-AuNWs electrode for 1 week. Figure S9 in the Supporting Information shows that the current responses to H_2O_2 maintain at the same level for the one-week duration with an RSD of only 1.3%.

We further examined the specificity of our biosensors by adding commonly used interferent species including 1.0 mM urea acid (UA), 1.0 mM ascorbic acid (AA), and 1.0 mM glucose (Glu). Figure 3D presents that the v-AuNWs electrode responses to a successive addition of 0.5 mM H_2O_2 while showing negligible responses to other three interferences at a concentration of 1 mM at the potential of −0.3 V. This result indicates a satisfactory selectivity of the v-AuNWs biosensor to H_2O_2 against these physiological electroactive species. Figure S10 in the Supporting Information displays a comparison of chronoamperometric responses to a successive addition of H_2O_2 with or without the presence of O_2. Although O_2 may also be reduced at similar potentials, it mainly influences the baseline current of the chronoamperometric responses rather than affects the detection of H_2O_2 at the ambient conditions, where O_2 concentration is constant.

Real-Time and In Situ Monitoring of H_2O_2 from Living Cells. In order to evaluate the feasibility of the v-AuNWs electrode in the detection of H_2O_2 released from living cells, MDA-MB-231 cells were cultured on the presterilized v-AuNWs electrode. Figure 4A shows the phase-contrast image of the cells seeded on the electrode after 24 h. Together with two more microscopic images of the cells on the electrode at higher magnification (Figure S11A and S11B), we could see the typical spindle-shaped cells adhered to the electrode. To further examine the biocompatibility of the electrode, the live/dead assay was conducted for the cells cultured on the presterilized v-AuNWs/PDMS patch 24 h after seeding. Obviously, majority of cells were alive, as stained by Calcein-AM (green), while negligible cells were dead, as stained by PI (red). These results clearly demonstrated excellent biocompatibility of our v-AuNWs electrodes to support the adhesion and growth of the mammalian cells.

The v-AuNWs electrode was further employed to monitor H_2O_2 from the living cells. PMA is a commonly used stimulus to induce the release of H_2O_2 from living cells.[8] Upon the stimuli of PMA, a series of signaling pathways will be activated. Along with the oxidation of O_2 by NADPH oxidase, free radical anion O_2^- will be generated. Under the catalysis of superoxide dismutases, H_2O_2 as the final product will be produced and released to the extracellular environment (see Figures 4C and 4D).[1,21] Catalase is an enzyme that can be used to selectively scavenge H_2O_2.[34] Figure 4E shows that there is a distinctive current increase upon the addition of PMA at a final concentration of 500 ng/mL. However, no apparent current increase occurs after the addition of the same amount of PMA in the control group without cells. To verify that the above current increase was induced by H_2O_2, catalase was added, reaching a final concentration of ~1000 U/mL, together with PMA addition. One can see that the current first increases slightly but soon falls back to its baseline level. The above results demonstrate specific detection of the H_2O_2 released from MDA-MB-231 cells cultured therein.

It is important to further examine whether the H_2O_2 can be detected in real time and in situ when the living cells are being stretched. To test this, 20% cyclic strains were applied on the electrode bearing MDA-MB-231 cells. An obvious current increase was still observed upon adding PMA during the stretch-release cycles (Figure 4F), indicating that detection of H_2O_2 induced by chemical stimulus was not influenced by mechanical deformation. We also observed a minor current increase upon the mechanical strains applied, which indicate cells might also release H_2O_2 in response to mechanical strain. However, this only slightly shifted the background and did not affect detection of PMA-induced H_2O_2. Further cellular morphological studies via optical microscopy and confocal microscopy show that cells were still adhered to the v-AuNWs electrode and alive without any observable damage or detachment under a mechanical strain of <50% (see Figures S11C, S11D, S12, and S13 in the Supporting Information).

■ CONCLUSIONS

In summary, we demonstrate that v-AuNWs can serve as intrinsically stretchable electrochemical biosensing platform toward cell analysis in real time and in situ. Unlike traditional rigid electrochemical electrodes, v-AuNWs offer higher electroactive surface areas, leading to a wider sensing window in the H_2O_2 model analyte system. This, in conjunction with biocompatibility, allows conformal cell growth on v-AuNWs with excellent adhesion. During mechanical stretching, no cell detachment or damage can be observed. These attributes enable the detection of H_2O_2 release from living cells under both nonstrained and strained states. We expect our

DOI: 10.1021/acs.analchem.9b02610
Anal. Chem. XXXX, XXX, XXX−XXX

stretchable v-AuNWs/PDMS electrochemical electrode may serve as a powerful and general platform for detecting other redox species related to cell metabolism.

■ ASSOCIATED CONTENT

Supporting Information

The Supporting Information is available free of charge on the ACS Publications website at DOI: 10.1021/acs.analchem.9b02610.

Additional information, including Figures S1−S13 and Table S1PDF)

■ AUTHOR INFORMATION

Corresponding Author

*E-mail: wenlong.cheng@monash.edu.

ORCID

Wenlong Cheng: 0000-0002-2346-4970

Notes

The authors declare no competing financial interest.

■ ACKNOWLEDGMENTS

This work is financially supported by ARC Discovery (Project Nos. DP170102208 and DP180101715). This work was performed in part at the Melbourne Centre for Nanofabrication (MCN) in the Victorian Node of the Australian National Fabrication Facility (ANFF).

■ REFERENCES

(1) Rhee, S. G. *Science* **2006**, *312* (5782), 1882−1883.
(2) Miller, E. W.; Dickinson, B. C.; Chang, C. J. *Proc. Natl. Acad. Sci. U. S. A.* **2010**, *107* (36), 15681−15686.
(3) Noh, J.; Kwon, B.; Han, E.; Park, M.; Yang, W.; Cho, W.; Yoo, W.; Khang, G.; Lee, D. *Nat. Commun.* **2015**, *6*, 6907.
(4) Liu, H.; Weng, L.; Yang, C. *Microchim. Acta* **2017**, *184* (5), 1267−1283.
(5) Kamsler, A.; Segal, M. *Mol. Neurobiol.* **2004**, *29* (2), 167−178.
(6) Trachootham, D.; Alexandre, J.; Huang, P. *Nat. Rev. Drug Discovery* **2009**, *8* (7), 579−591.
(7) Mandoli, C.; Pagliari, F.; Magnani, E.; Licoccia, S.; Forte, G.; Di Nardo, P.; Pagliari, S.; Minieri, M.; Nardone, G.; Traversa, E. *ACS Nano* **2012**, *6* (5), 3767−3775.
(8) Wu, P.; Qian, Y.; Du, P.; Zhang, H.; Cai, C. *J. Mater. Chem.* **2012**, *22* (13), 6402−6412.
(9) Zhang, Y.; Wu, C.; Zhou, X.; Wu, X.; Yang, Y.; Wu, H.; Guo, S.; Zhang, J. *Nanoscale* **2013**, *5* (5), 1816−1819.
(10) Zhang, Y.; Bai, X.; Wang, X.; Shiu, K. K.; Zhu, Y.; Jiang, H. *Anal. Chem.* **2014**, *86*, 9459−9465.
(11) Xi, F.; Zhao, D.; Wang, X.; Chen, P. *Electrochem. Commun.* **2013**, *26* (1), 81−84.
(12) Bai, J.; Jiang, X. *Anal. Chem.* **2013**, *85* (17), 8095−8101.
(13) Lubarsky, G.; Zhu, Z.; Li, M.; Papakonstantinou, P.; Lin, J.; Zhu, H.; Wang, T.; Zhuo, J. *Anal. Chem.* **2013**, *85* (21), 10289−10295.
(14) Wang, N.; Han, Y.; Xu, Y.; Gao, C.; Cao, X. *Anal. Chem.* **2015**, *87* (1), 457−463.
(15) Wu, Y.; Xiao, F.; Liu, H.; Dong, S.; Xi, J.; Liu, H.; Fu, C. *Anal. Chim. Acta* **2015**, *853*, 200−206.
(16) Jin, D.; Xiao, X.; Xu, J.; Pang, H.; Hu, X.; Shu, Y.; Chen, J.; Xu, Q. *Sens. Actuators, B* **2017**, *252*, 72−78.
(17) Rui, Q.; Komori, K.; Tian, Y.; Liu, H.; Luo, Y.; Sakai, Y. *Anal. Chim. Acta* **2010**, *670* (1−2), 57−62.
(18) Sun, Y.; He, K.; Zhang, Z.; Zhou, A.; Duan, H. *Biosens. Bioelectron.* **2015**, *68*, 358−364.
(19) Li, X.; Liu, Y.; Zhu, A.; Luo, Y.; Deng, Z.; Tian, Y. *Anal. Chem.* **2010**, *82* (15), 6512−6518.
(20) Sheng, Q.; Bai, W.; Zheng, J.; Zhang, S.; Zhang, X. *Sens. Actuators, B* **2017**, *242*, 718−727.
(21) Jiang, X.; Wang, H.; Yuan, R.; Chai, Y. *Anal. Chem.* **2018**, *90* (14), 8462−8469.
(22) Xiao, F.; Li, Y.; Zan, X.; Liao, K.; Xu, R.; Duan, H. *Adv. Funct. Mater.* **2012**, *22* (12), 2487−2494.
(23) Zhao, X.; Wang, K.; Li, B.; Wang, C.; Ding, Y.; Li, C.; Mao, L.; Lin, Y. *Anal. Chem.* **2018**, *90* (12), 7158−7163.
(24) Liu, Y. L.; Jin, Z. H.; Liu, Y. H.; Hu, X. B.; Qin, Y.; Xu, J. Q.; Fan, C. F.; Huang, W. H. *Angew. Chem., Int. Ed.* **2016**, *55* (14), 4537−4541.
(25) Liu, Y. L.; Qin, Y.; Jin, Z. H.; Hu, X. B.; Chen, M. M.; Liu, R.; Amatore, C.; Huang, W. H. *Angew. Chem., Int. Ed.* **2017**, *56* (32), 9454−9458.
(26) Wang, Y. W.; Liu, Y. L.; Xu, J. Q.; Qin, Y.; Huang, W. H. *Anal. Chem.* **2018**, *90* (10), 5977−5981.
(27) Zhu, B.; Gong, S.; Cheng, W. *Chem. Soc. Rev.* **2019**, *48*, 1668−1711.
(28) Zhu, B.; Gong, S.; Lin, F.; Wang, Y.; Ling, Y.; An, T.; Cheng, W. *Adv. Electron. Mater.* **2019**, *5* (1), 1800509.
(29) An, T.; Ling, Y.; Gong, S.; Zhu, B.; Zhao, Y.; Dong, D.; Yap, L. W.; Wang, Y.; Cheng, W. *Adv. Mater. Technol.* **2019**, *4* (3), 1800473.
(30) Wang, Y.; Gong, S.; Wang, S. J.; Yang, X.; Ling, Y.; Yap, L. W.; Dong, D.; Simon, G. P.; Cheng, W. *ACS Nano* **2018**, *12* (10), 9742−9749.
(31) Zhai, Q.; Wang, Y.; Gong, S.; Ling, Y.; Yap, L. W.; Liu, Y.; Wang, J.; Simon, G. P.; Cheng, W. *Anal. Chem.* **2018**, *90* (22), 13498−13505.
(32) Zhai, Q.; Gong, S.; Wang, Y.; Lyu, Q.; Liu, Y.; Ling, Y.; Wang, J.; Simon, G. P.; Cheng, W. *ACS Appl. Mater. Interfaces* **2019**, *11*, 9724−9729.
(33) Trasatti, S.; Petrii, O. A. *Pure Appl. Chem.* **1991**, *63* (5), 711−734.
(34) Szymczyk, K. H.; Kerr, B. A. E.; Freeman, T. A.; Adams, C. S.; Steinbeck, M. J. *Biochem. Pharmacol.* **2006**, *72* (6), 761−769.

DOI: 10.1021/acs.analchem.9b02610
Anal. Chem. XXXX, XXX, XXX−XXX